Letter

Novel isoxazole derivatives with potent FXR agonistic activity prevent acetaminophen induced liver injury

Valentina Sepe, Silvia Marchianò, Claudia Finamore, Giuliana Baronissi, Francesco Saverio Di Leva, Adriana Carino, Michele Biagioli, Chiara Fiorucci, Chiara Cassiano, Maria Chiara Monti, Federica Del Gaudio, Ettore Novellino, Vittorio Limongelli, Stefano Fiorucci, and Angela Zampella

ACS Med. Chem. Lett., **Just Accepted Manuscript** • DOI: 10.1021/acsmedchemlett.8b00423 • Publication Date (Web): 06 Dec 2018

Novel isoxazole derivatives with potent FXR agonistic activity prevent acetaminophen induced liver injury

Valentina Sepe,[1] Silvia Marchianò,[2] Claudia Finamore,[1] Giuliana Baronissi,[1] Francesco Saverio Di Leva[1§], Adriana Carino,[2] Michele Biagioli,[2] Chiara Fiorucci,[2] Chiara Cassiano,[4] Maria Chiara Monti,[4] Federica del Gaudio,[4] Ettore Novellino,[1] Vittorio Limongelli,[1,3] Stefano Fiorucci[2§] and Angela Zampella[1§*]

[1]Department of Pharmacy, University of Naples "Federico II", via D. Montesano 49, 80131 Naples, Italy.

[2]Department of Surgery and Biomedical Sciences, Nuova Facoltà di Medicina, Perugia, Italy

[3]Università della Svizzera Italiana (USI), Faculty of Biomedical Sciences, Institute of Computational Science - Center for Computational Medicine in Cardiology, Via G. Buffi 13, CH-6900 Lugano, Switzerland.

[4]Department of Pharmacy, University of Salerno, Via Giovanni Paolo II, 132, 84084, Fisciano, Salerno, Italy.

KEYWORDS: *FXR agonists, bile acid receptors, trisubstituted isoxazole scaffold, liver diseases, acetaminophen, hepatotoxicity.*

ABSTRACT: Acetaminophen misuse is a leading cause of acute liver failure and liver transplantation for which therapy is poorly effective. FXR ligands have shown effective in reducing liver injury in several experimental and clinical settings. In this report, we have elaborated on the structure of GW4064, the first non-steroidal agonist for FXR, to identify novel isoxazoles endowed with FXR agonistic activity and improved ADME properties. The pharmacological characterization and molecular docking studies for the structure-activity rationalization allowed the identification of several FXR agonists with nanomolar potency in transactivation and SRC-1 recruitment assays. This characterization resulted in the identification of a potent FXR agonist, compound **20** that was orally active, and rescued mice from acute liver failure caused by acetaminophen overdose in a FXR-dependent manner.

Apart from their function in facilitating the absorption of dietary lipids by the small intestine, bile acids regulate their own synthesis, secretion, transport, storage, metabolism, and toxicity, by activating a family of receptors known as bile acid activated receptors. This family includes both G-protein coupled receptors and nuclear receptors such as the farnesoid X receptor (FXR). FXR is a bile acid sensor, with primary bile acids, i.e. chenodeoxycholic acid (CDCA, **1**) in humans, and cholic acid (CA) in mouse, and the corresponding taurine or glycine amide conjugates (Figure 1A), serving as natural ligands.[1,2]

FXR is expressed by entero-hepatic tissues including liver, gallbladder, intestine, and by the kidney, governing bile acid homeostasis by repressing bile acid synthesis and uptake while increasing their urinary excretion, as protective mechanism in conditions of impaired biliary excretion (cholestasis).[3] In addition, FXR activation plays functional roles in regulating glucose[4] and lipid metabolism[5,6] and exerting robust anti-inflammatory activity in intestine[7] and in the liver,[8] and is considered a validated target for the treatment of liver diseases, such as cholestasis, liver fibrosis,[9] steatohepatitis (NASH),[10,11] diabetes,[12] as well as obesity,[13] metabolic syndrome,[14] and inflammatory bowel disease.[15]

Hence, FXR agonists are of great pharmacological interest and several small molecule agonists have been described.[16,17,18]

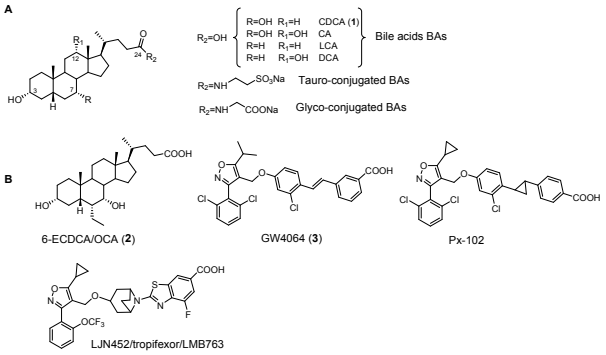

Figure 1. A) Endogenous bile acids; B) FXR agonists in advanced clinical trials

These molecules cover diverse chemical spaces that should be included in two large families, steroidal and non-steroidal scaffolds. Figure 1B highlights FXR agonists currently in advanced pre-clinical and clinical trials. Within the two above mentioned families, the semisynthetic CDCA derivative obeticholic acid (INT747/6-ECDCA/OCA, **2**),[19] represents the first-in-class of FXR ligands approved for the treatment of UDCA-resistant patients with primary biliary cholangitis (PBC), recently progressed in Phase III trials on NASH patients.

On the other hand, GW4064 (**3**) is a first in class of non-steroidal FXR ligands representing the prototype of isoxazole-type FXR agonists[20] endowed with an efficacy of 140% *versus* CDCA. Several reports over the years have elaborated on the GW4064 chemical space to address the limited bioavailability as well as the stilbene-mediated photo-instability. Thus, medicinal chemistry protocols have been mainly focused on the linker between the largely conserved trisubstituted isoxazole core and the terminal acidic entity, affording to the identification of a large family of isoxazole derivatives.[16,17] Among these, Px-102 and LJN452 (tropifexor, LMB763),[21,22] with a trans-cyclopropyl and an 8-azabicyclo[3.2.1]-octane ring as linker, respectively, represent elegant solutions to the poor GW4064 ADME profile. Both molecules have recently progressed into Phase II clinical trial in patients with NASH.

The challenge of the present work is to find novel isoxazole-type FXR agonists of similar efficacy with the additional requirement of improved ADME properties. Thus, several modifications have been introduced on the oxymethylene at C-4 while maintaining the central isoxazole core, with the isopropyl group at C-5 and the 2,6-dicloro-substituted phenyl moiety at C-3. The structures of the newly identified FXR agonists are shown in Table 1. Pharmacological experiments resulted in the identification of several compounds endowed with selective agonistic activity toward FXR and notably to the identification of compound **20**, which combines the good pharmacokinetic properties with the distinct ability to specifically bind and regulate FXR activity *in vivo*, and to rescue mice from acute liver failure caused by acetaminophen overdose in a FXR-dependent manner.

The synthetic procedures for the preparation of compounds **4-24** and Scheme S1 are reported and detailed in the Supplementary Information (SI).

FXR agonistic activities are reported in Table 1. Efficacy of compounds **4-24** was firstly evaluated on FXR in a cell-free Alpha Screen assay in comparison with reference compounds **1-3**.

First, fragmentation of GW4064 (**3**) structure resulted in a general drop in activity respect to 6-ECDCA and GW4064 with dramatic effects operated by the presence of the carboxyl group on the terminal aromatic group (compounds **8** and **13**).

In contrast, nitrile **6** and alcohol **7** exhibited similar activity to GW4064. The efficacy of compounds **6** and **7** is highly influenced by the position of the non-acidic substituent on the terminal aromatic ring (compare **6** *vs* **13** and **7** *vs* **12**) with *p*-substituted derivatives showing a comparable efficacy than GW4064 in SRC-1 recruitment assay (see Table 1).

Of interest, in the above subset of simplified derivatives, the replacement of the COOH moiety with the methyl sulfonate isoster produces compound **9**, with a promising efficacy (167% *vs* **1**, 109% *vs* **2**) and, thus, opening up, in this class of molecules, possibilities for minimizing phase II metabolism in vivo. Elongation at C-4 isoxazole chemical space by introduction of an additional substituted aromatic ring resulted in an opposite behavior with the carboxylic group on the terminal aryl moiety resulting a mandatory hallmark for effective FXR agonists. In a cross comparison between the carboxylic acid bearing derivatives, the exact position of the acid moiety on the terminal aromatic ring produces a negligible effect on SRC-1 recruitment with the *meta*-derivative **24** slightly more effective than the *para* isomer **20**. Of interest, the above efficacy in SRC-1 recruitment is not affected by the conformational freedom around the two aromatic rings with the constrained derivative **16** showing comparable efficacy than compound **24**.

Alpha Screen results were confirmed by transactivation assay on HepG2 cells transiently transfected with hFXR with the relative potency of all series investigated by a detailed measurement of concentration-response curves. As reported in Table 1, the best match in term of efficacy and potency outcomes for compounds **6**, **16**, **20** and **24**, with compound **20** as the most potent derivative found in this screening (EC_{50} 0.30±0.006 μM, efficacy 149%). Besides, even if less potent than GW4064 in FXR transactivation, these compounds showed a similar efficacy in SRC-1 recruitment with respect of GW4064 as reported in Table 1. Thus, compound **20** represents the most promising compound of the series considering its efficacy in the recruitment of the coactivator SRC-1 very close to GW4064 (Table 1) and pharmacokinetics profile (see below for details).

Table 1. FXR agonistic activity of 4-24

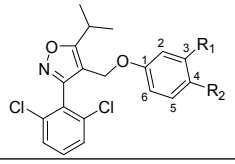

Compound	R_1	R_2	Eff (% Ref.)[a]		EC_{50}[b]
			vs CDCA	*vs* ECDCA	
CDCA (1)	-	-	-	61±16	20
6-ECDCA **(2)**	-	-	165±7	-	0.5
GW4064 **(3)**	-	-	166±15	101±15	0.02
4	H	H	114±7	69±7	1.59±0.35
5	H	COOMe	136±7	83±7	3.59±1.08
6	H	CN	151±6	92±6	0.81±0.20
7	H	CH_2OH	164±18	100±8	2.93±1.09
8	H	COOH	43±18	26±18	6.67±1.7
9	H	SO_2CH_3	167±7	102±7	1.09±0.1
10	COOMe	H	120±6	73±6	2.06±0.26
11	CN	H	93±17	56±17	10.17±0.84
12	CH_2OH	H	76±20	46±20	4.37±0.72

13	COOH	H	67±18	40±18	19.74±0.31
14	H	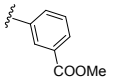	125±3	64±3	2.8±0.36
15	H	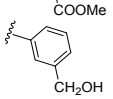	121±2	61±2	0.83±0.06
16	H	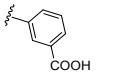	175±3	115±3	1.4±0.32
17	H	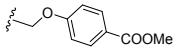	92±1	56±1	0.73±0.07
18	H	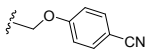	83±2	50±2	0.94±0.02
19	H	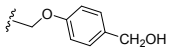	103±4	63±4	0.74±0.02
20	H	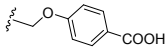	149±12	91±13	0.30±0.006
21	H	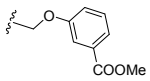	97±3	36±3	1.15±0.37
22	H	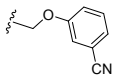	117±5	56±5	5.4±0.51
23	H	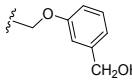	124±14	63±14	0.67±0.038
24	H	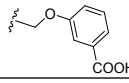	191±4	130±4	0.46±0.033

[a]Alpha Screen coactivator recruitment assay measuring a direct interaction of FXR with SRC-1; ligands were tested at 5 μM. Eff (%) is the maximum efficacy of the compound relative to CDCA and/or 6-ECDCA set alternatively as 100%. Results are expressed as mean of three independent measurements ± standard error. [b]Transactivation assays on HepG2 cells. EC_{50} values (μM) were calculated from at least three experiments. Results are expressed as mean ± SEM.

Therefore, we have decided to perform docking studies to shed light on its binding mode to the ligand binding domain (LBD) of FXR. The most occurring top scored docking pose shows that the ligand's 3-(2,6-dichlorophenyl)-5-isopropylisoxazole moiety occupies the hydrophobic cavity of the LBD defined by helices H3, H5, H6, H7, H11 and H12 (Figure 2A). Herein, the ligand engages favorable van der Waals contacts with the residues Phe284, Leu287, Phe329, Ile352, Trp454, and Leu465. In addition, the isoxazole ring forms a hydrogen bond with the protonated His447 of H10 and π-stacking interactions with Trp469 of H12. These ligand/protein interactions are able to stabilize in the LBD of FXR the cation-π interaction formed by the latter two residues (i.e., His447 and Trp469) that has been reported to favor the receptor conformation responsible for the recruitment of the coactivator partner, activating gene transcription.[23,24,25] On the other side of the binding site, the carboxylic group of compound **20** H-binds with the backbone atoms of Met265 and forms a salt bridge with the side chain of Arg331 at H5. The latter is the strongest interaction between **20** and FXR, thus acting as ligand anchor point in the LBD. It is worth noting that a similar ionic interaction with Arg331 has been previously reported to stabilize the binding of bile acid derivatives to FXR.[23] Finally, the ligand's *p*-(phenoxymethyl)phenoxymethyl linker forms a number of hydrophobic contacts with residues such as Met265, Leu287, Met290, Ile335, and Ile352, contributing to stabilize the ligand binding conformation.

The elucidation of the binding mode of **20** allowed the rationalization of the different efficacy values of the other derivatives of the series reported in Table 1. From the structural point of view, the compounds of the series differ for the distance of the isoxazole ring from the terminal functional group and the nature of the latter. Compounds endowed with the biphenyloxymethyl and the *p*-(phenoxymethyl)phenoxymethyl linker like compound **20** and presenting diverse terminal groups such as –COOH, $–CH_2OH$, $–COOCH_3$ and –CN, can similarly interact with Arg331 thanks to both the flexibility of the ligand's linker and the arginine side chain (see Figure S1).

As a result, the derivatives with *para* and *meta* substituted terminal groups display comparable efficacy (i.e., **20** *vs* **24**). However, less polar terminal functional groups like $–COOCH_3$ (**9** and **21**) weaken the interaction with Arg331, thus reducing the ligand-induced recruitment of the coactivator (i.e., lower efficacy). On the other hand, the terminal functional group of compounds endowed with the shorter phenoxymethyl linker (**4** to **8**, **10** to **13**, and **8**) poorly interacts with Arg331, while it is placed close by hydrophobic residues like Ile335, Met265 and Met290 and the polar His294 (see Figure S2). This explains why in these compounds the presence of polar but not charged terminal functional groups leads to ligands with higher efficacy (see **5**, **6**, **7** and **9** *vs* **8**).

Finally, considering the structural similarity between **20** and GW4064, we deemed important to compare the docking pose of **20** with the X-ray binding conformation of GW4064.[23] The overlap of the two binding modes in the LBD of FXR shows a common pattern of interaction with the receptor in which the

two ligands similarly occupy the LBD, thus allowing the proper interaction with His447 and Arg331 (Figure 2B).
The physicochemical parameters of a subset of the above mentioned analogs were assessed by LC-MS analysis (Table 2).

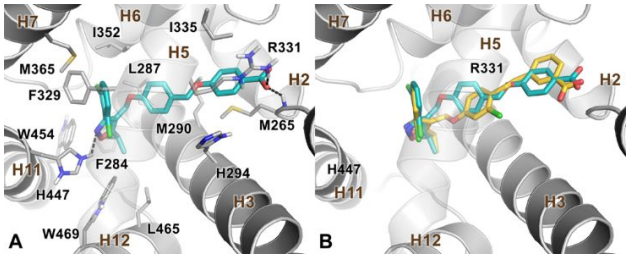

Figure 2. (A) Docking pose of **20** (cyan sticks) in the FXR LBD crystal structure. The receptor is shown as gray ribbons, with amino acids important for ligand binding highlighted as sticks. Non polar hydrogens are omitted for clarity. Hydrogen bonds are shown as dashed black lines. (B) Superposition between the predicted binding mode of **20** and the crystallographic pose of GW4064 (yellow sticks).

As expected, compound **6** suffers of very low aqueous solubility, whereas **9** gains in polarity respect to GW4064 (**3**). The comparison between the carboxylic acid derivatives **16**, **20** and **24**, isomeric for the position of the carboxylic unit on the terminal aromatic ring is of interest. Compound **24**, bearing the acid in the 3-position relative to the oxymethylene linker, as well as the corresponding constrained derivative **16**, exhibited improved aqueous solubility compared to the corresponding 4-position isomer, compound **20**.
These results were further challenged by assessing the metabolic stability by *in vitro* incubation with rat liver microsomes. Compounds **16**, **20** and **24** showed moderate clearances, significantly lower than the starting lead GW4064 (**3**) and the steroidal reference compound 6-ECDCA (**2**), with half-lives greater than 1 h for compounds **20** and **24**.

Table 2. *In vitro* pharmacokinetics for selected derivatives

Compound	Solubility[a] (μM)	Cl_{int}[b]	$t_{½}$ (min)	%[c]
6-ECDCA **(2)**	>200	109	21	27
GW4064 **(3)**	152	56	41	48
6	3	299	8	3
9	>200	112	21	26
16	75	53	44	56
20	44	32	72	67
24	>200	35	66	62

[a]Aqueous solubility at pH 7.4; [b]Reported as μL/min/mg protein; [c]Percentage of compound remaining in solution after 40 min incubation. Each measurement has been repeated in triplicate and SD < 5%.

Finally, compounds **6** and **9** showed a very low metabolic stability *in vitro,* with only 3% and 26% of unmodified molecule remaining after 40 min, respectively, and these data rule out the pharmacological potential of these compounds.
To gain insights into the agonism and to support target engagement for compounds **16**, **20** and **24**, the effect in modulating SHP, a FXR target gene, was assessed in a liver carcinoma cell line HepG2 by RT-PCR, with GW4064 (10 μM) as reference compound. Among the three selected hits, compounds **20** and **24** at 5 μM concentration were more potent than GW4064 in the induction of SHP mRNA expression (Figure S3 in the SI). Because this gene is endowed with a canonical FXR-responsive element in the promoter, this result is fully consistent with the nature of compounds **20** and **24** as potent FXR agonists. Of interest, the above potency is independent from the position of the carboxylic unit on the terminal aromatic ring. Further, the *in vitro* profile of compounds **20** and **24** was expanded to common off targets for bile acid receptor ligands. Compounds **20** and **24** were unable to induce LXRα/LXRβ and PPARγ transactivation on HepG2 cells (Figure S3, SI). Moreover, compounds **4-24** were demonstrated inactive toward GPBAR1 (Figure S4, SI).
Collectively, compound **20** combines the high efficacy in the recruitment of SRC-1 at FXR, fully comparable to GW4064 (Table 1), with an excellent metabolic stability (Table 2), while the low aqueous solubility might raise concerns over its oral bioavailability *in vivo*. Thus, to evaluate the *in vivo* intestinal absorption, mice were administered with compound **20** for three days by o.s. or by i.p and hepatic expression of target genes, i.e. SHP and BSEP, measured by RT-PCR.

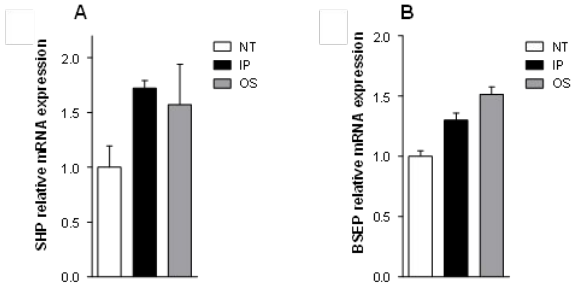

Figure 3. Mice were administered with 10 mg/kg of **20**, daily by gavage (o.s.) or i.p. for 3 days. Total RNA extracted from liver was used to evaluate by quantitative real-time PCR the relative mRNA expression of (A) SHP and (B) BSEP. The data are normalized to GADPH mRNA. Results are the mean ± SEM of four mice per group.

The data shown in Figure 3 demonstrate that both genes were upregulated following administration of **20** either by o.s or by i.p., thus demonstrating that **20** is absorbed in the intestine and transported to the liver.
In vivo acetaminophen (APAP) liver toxicity. APAP is one of the most prescribed drugs worldwide. Though safe at therapeutic doses, APAP overdosing causes severe liver injury which results in acute liver failure.[26] Currently, APAP overdose is the leading cause of acute liver failure in the United States and most of Europe and represents a major indication for liver transplantation. At therapeutic doses, APAP is metabolized in the liver by phase II conjugation enzymes and transformed in the corresponding sulfate and glucoronate derivatives, with only a small amount being converted into the cytotoxic Michael acceptor *N*-acetyl-*p*-quinoneimine (NAPQI), which in turn is rapidly detoxified by glutathione (GSH) conjugation. However, excessive NAPQI formation, resulting from APAP overdose, saturates phase II conjugation pathways, leading to formation of large amounts of the toxic NAPQI metabolite,[27] depletion of hepatic GSH and binding to cellular proteins with consequently increased oxidative stress and mitochondrial damage. Because therapy for APAP-induced acute liver toxicity remains

suboptimal, we have decided to investigate whether FXR agonism might rescue from acute liver failure caused in mice

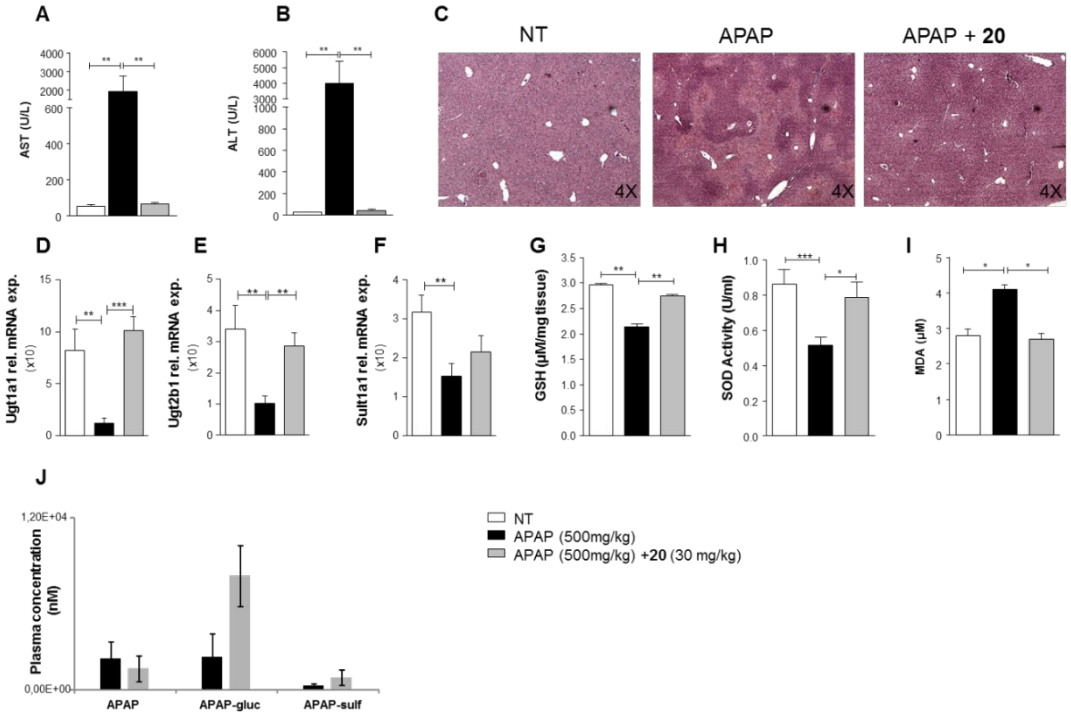

by APAP overdosing. For this purpose, C57Bl6 mice were administered a single dose of 500 mg/kg APAP.

Figure 4. Compound **20** rescues mice form acute liver injury caused by APAP overdose. Serum levels of (A) AST and (B) ALT; (C) Hematoxylin and eosin (H&E) staining on mice liver tissues; Relative mRNA levels of (D) Ugt1a1, (E) Ugt2b1 and (F) Sult1a1 in liver; (G) Hepatic levels of GSH, (H) Hepatic SOD Activity and (I) Hepatic levels of MDA; (J) Effects of **20** APAP metabolic disposition with mouse plasma contents (nM) of APAP, APAP-glucuronide and APAP-sulfate. Each value represents the mean ± SEM of 5-8 animals per group.*p < 0.01.

Twenty four hours later, surviving mice were sacrificed and blood and liver sections collected. As illustrated in Figure 4A-B, while treating mice with APAP resulted in a severe liver injury with ~50 fold increase of AST and ALT plasma levels ($p<0.01$ versus naïve mice), this pattern was completely reversed by treating mice with compound **20** at the dose of 30 mg/kg ($p<0.01$ versus APAP alone). A similar pattern of protection was observed in mice administered GW4064 (data not shown). At the histopathology analysis we found that compound **20** was highly effective in rescuing mice from liver necrosis caused by APAP (Figure 4C). To gain insights on the molecular mechanism that supports protection afforded by compound **20**, we have then examined the effect that this agent on enzymes involved in xenobiotic metabolism.[28] As shown in Figure 4D-F, exposure to APAP results in a dramatic downregulation of the expression of glucuronosyltransferases (Ugt1a1 and Ugt2b1) and sulfotransferase family 1A member 1 (Sult1a1) ($p<0.01$). These three genes encode for Phase II enzymes involved in xenobiotics detoxification and are known for being FXR regulated genes. The results of these investigations demonstrated that compound **20** effectively restores the expression of Phase II genes. Consistent with these findings, compound **20** effectively reestablished the liver levels of glutathione and super-oxide dismutase (SOD) (Figure 4G and H, $p<0.01$). In addition, compound **20** reduced the level of lipid peroxidation in mice administered with APAP, as indicated by changes of malonildialdehyde (MDA) levels in the liver of various experimental groups (Figure 5I, $p<0.01$).

APAP and its main Phase II conjugates (APAP-glucoronate and APAP-sulfate) in plasma were measured by LC-MS/MS and the relative concentrations are shown in Figure 5J. Plasma APAP concentration reached ~1000 nM, in response to APAP treatment. Treatment with compound **20** slightly decreased APAP plasma concentration (615 nM) while enhanced the concentration of APAP metabolites, APAP-glucuronide and APAP-sulfate, thereby indicating that compound **20** increases APAP metabolism by the liver.

In conclusion, in this report, elaboration on GW4064 chemical space afforded the identification of several FXR agonists with nanomolar potency in transactivation and SRC-1 recruitment assays. This study resulted in the identification of compound **20**, an orally active FXR agonist that rescues mice from acute toxicity caused by APAP.

ASSOCIATED CONTENT

Supporting Information

The Supporting Information is available free of charge on the ACS Publications website.

Synthesis, experimental procedures, docking poses of **9**, **16** and **24** in FXR-LBD, Figure S3 and S4, ^{1}H and ^{13}C NMR of compounds **4-24** (PDF).

AUTHOR INFORMATION

Corresponding Author

*Prof. Angela Zampella; e-mail: angela.zampella@unina.it

Author Contributions

[§]These authors equally contributed to this work

Notes

The authors declare no competing financial interest.

ACKNOWLEDGMENT

This work was supported by a grant from University of Naples Federico II "Finanziamento della Ricerca in Ateneo (DR/2016/341, February 2016)" and the Swiss National Science Foundation (Project N. 200021_163281). V.L. also thanks the COST action CA15135 (Multi-target paradigm for innovative ligand identification in the drug discovery process MuTaLig) for the support.

ABBREVIATIONS

ADME, absorption, distribution, metabolism, and excretion; APAP, Acetaminophen; CDCA, chenodeoxycholic acid; Cl_{int}, intrinsic clearance; FXR-LBD, Farnesoid X Receptor, Ligand Binding Domain; GPBAR1, membrane G-protein coupled bile acid receptor; GSH, glutathione; LXRα/LXRβ, liver X receptor α or β; NAPQI, N-acetyl-p-quinoneimine; NASH, Nonalcoholic steatohepatitis; PPARγ, Peroxisome proliferator-activated receptor gamma; SRC-1, steroid receptor coactivator-1.

REFERENCES

(1) Makishima, M.; Okamoto, A. Y.; Repa, J. J.; Tu, H.; Learned, R. M.; Luk, A.; Hull, M. V.; Lustig, K. D.; Mangelsdorf, D. J.; Shan, B. Identification of a nuclear receptor for bile acids. *Science* **1999**, *284*, 1362-1365.

(2) Parks, D. J.; Blanchard, S. G.; Bledsoe, R. K.; Chandra, G.; Consler, T. G.; Kliewer, S. A.; Stimmel, J. B.; Willson, T. M.; Zavacki, A. M.; Moore, D. D.; Lehmann, J. M. Bile acids: natural ligands for an orphan nuclear receptor. *Science* **1999**, *284*, 1365-1368.

(3) Stedman, C.; Liddle, C.; Coulter, S.; Sonoda, J.; Alvarez, J. G.; Evans, R. M.; Downes, M. Benefit of farnesoid X receptor inhibition in obstructive cholestasis. *Proc. Natl. Acad. Sci.* USA **2006**, *103*, 11323-11328.

(4) Zhang, Y.; Lee, F. Y.; Barrera, G.; Lee, H.; Vales, C.; Gonzalez, F. J.; Willson, T. M.; Edwards, P. A. Activation of the nuclear receptor FXR improves hyperglycemia and hyperlipidemia in diabetic mice. *Proc. Natl. Acad. Sci.* USA **2006**, *103*, 1006-1011.

(5) Cipriani, S.; Mencarelli, A.; Palladino, G.; Fiorucci, S. FXR activa-tion reverses insulin resistance and lipid abnormalities and protects against liver steatosis in Zucker (fa/fa) obese rats. *J. Lipid Res*. **2010**, *51*, 771-784.

(6) Sinal, C. J.; Tohkin, M.; Miyata, M.; Ward, J. M.; Lambert, G.; Gonzalez, F. J. Targeted disruption of the nuclear receptor FXR/BAR impairs bile acid and lipid homeostasis. *Cell* **2000**, *102*, 731-744.

(7) Inagaki, T.; Moschetta, A.; Lee, Y. K.; Peng, L.; Zhao, G.; Downes, M.; Yu, R. T.; Shelton, J. M.; Richardson, J. A.; Repa, J. J.; Mangelsdorf, D. J.; Kliewer, S. A. Regulation of antibacterial defense in the small intestine by the nuclear bile acid receptor. *Proc. Natl. Acad. Sci.* USA. **2006**, *103*, 3920-3925.

(8) Huang, W.; Ma, K.; Zhang, J.; Qatanani, M.; Cuvillier, J.; Liu, J.; Dong, B.; Huang, X.; Moore, D. D. Nuclear receptor-dependent bile acid signaling is required for normal liver regeneration. *Science* **2006**, *312*, 233-236.

(9) Fiorucci, S.; Antonelli, E.; Rizzo, G.; Renga, B.; Mencarelli, A.; Riccardi, L.; Orlandi, S.; Pellicciari, R.; Morelli, A. The nuclear receptor SHP mediates inhibition of hepatic stellate cells by FXR and protects against liver fibrosis. *Gastroenterology* **2004**, *127*, 1497-1512.

(10) Cariou, B. The farnesoid X receptor (FXR) as a new target in non-alcoholic steatohepatitis. *Diabetes Metab.* **2008**, *34*, 685-691.

(11) Fiorucci, S.; Cipriani, S.; Baldelli, F.; Mencarelli, A. Bile acid-activated receptors in the treatment of dyslipidemia and related disorders. *Prog. Lipid Res*. **2010**, *49*, 171-185.

(12) Mencarelli, A.; Renga, B.; D'Amore, C.; Santorelli, C.; Graziosi, L.; Bruno, A.; Monti, M. C.; Distrutti, E.; Cipriani, S.; Donini, A.; Fiorucci, S. Dissociation of intestinal and hepatic activities of FXR and LXRα supports metabolic effects of terminal ileum interposition in rodents. *Diabetes* **2013**, *62*, 3384-3393.

(13) Moschetta, A.; Bookout, A. L.; Mangelsdorf, D. J. Prevention of cholesterol gallstone disease by FXR agonists in a mouse model. *Nat. Med*. **2004**, *10*, 1352-1358.

(14) Cariou, B.; Staels, B. FXR: a promising target for the metabolic syndrome? *Trends Pharmacol. Sci.* **2007**, *28*, 236-243.

(15) Fiorucci, S.; Cipriani, S.; Mencarelli, A.; Renga, B.; Distrutti, E.; Baldelli, F. Counter-regulatory role of bile acid activated receptors in immunity and inflammation. *Curr. Mol. Med.* **2010**, *10*, 579-595.

(16) Gege, C.; Kinzel, O.; Steeneck, C.; Schulz, A.; Kremoser, C. Knocking on FXR's Door: the "hammerhead"-structure series of FXR agonists-amphiphilic isoxazoles with potent in vitro and in vivo activities. *Curr. Top. Med. Chem.* **2014**, *14*, 2143-2158.

(17) Xu Y. Recent progress on bile acid receptor modulators for treatment of metabolic diseases. *J. Med. Chem*. **2016**, *59*, 6553-6579.

(18) Sepe, V.; Distrutti, E.; Fiorucci, S.; Zampella, A. Farnesoid X receptor modulators 2014-present: a patent review. *Expert Opin. Ther. Pat.* **2018**, *28*, 351-364.

(19) Pellicciari, R.; Fiorucci, S.; Camaioni, E.; Clerici, C.; Costantino, G.; Maloney, P. R.; Morelli, A.; Parks, D. J.; Willson, T. M. 6-alpha-etyl-chenodeoxycholic acid (6-ECDCA), a potent and selective FXR agonist endowed with anticholestatic activity. *J. Med. Chem.* **2002**, *45*, 3569-3572.

(20) Maloney, P. R.; Parks, D. J.; Haffner, C. D.; Fivush, A. M.; Chandra, G.; Plunket, K. D.; Creech, K. L.; Moore, L. B.; Wilson, J. G.; Lewis, M.C.; Jones, S. A.; Willson, T. M. Identification of a chemical tool for the orphan nuclear receptor FXR. *J. Med. Chem.* **2000**, *43*, 2971-2974.

(21) Kinzel, O.; Steeneck, C.; Schlüter, T.; Schulz, A.; Gege, C.; Hahn, U.; Hambruch, E.; Hornberger, M.; Spalwisz, A.; Frick, K.; Perović-Ottstadt, S.; Deuschle, U.; Burnet, M.; Kremoser, C. Novel substituted isoxazole FXR agonists with cyclopropyl, hydroxycyclobutyl and hydroxyazetidinyl linkers: Understanding and improving key determinants of pharmacological properties. *Bioorg. Med. Chem. Lett.* **2016**, *26*, 3746-3753.

(22) Tully, D. C.; Rucker, P. V.; Chianelli, D.; Williams, J.; Vidal, A.; Alper, P. B.; Mutnick, D.; Bursulaya, B.; Schmeits, J.; Wu, X.; Bao, D.; Zoll, J.; Kim, Y.; Groessl, T.; McNamara, P.; Seidel, H. M.; Molteni, V.; Liu, B.; Phimister, A.; Joseph, S. B.; Laffitte, B. Discovery of tropifexor (LJN452), a highly potent non-bile acid FXR agonist for the treatment of cholestatic liver diseases and nonalcoholic steatohepatitis (NASH). *J. Med. Chem*. **2017**, *60*, 9960-9973.

(23) Mi, L. Z.; Devarakonda, S.; Harp, J. M.; Han, Q.; Pellicciari, R.; Willson, T. M.; Khorasanizadeh, S.; Rastinejad, F. Structural basis for bile acid binding and activation of the nuclear receptor FXR. *Mol. Cell* **2003**, *11*, 1093-1100.

(24) Di Leva, F. S.; Festa, C.; D'Amore, C.; De Marino, S.; Renga, B.; D'Auria, M. V.; Novellino, E.; Limongelli, V.; Zampella, A.; Fiorucci, S. Binding mechanism of the farnesoid X receptor marine antagonist suvanine reveals a strategy to forestall drug modulation on nuclear receptors. Design, synthesis, and biological evaluation of novel ligands. *J. Med. Chem*. **2013**, *56*, 4701-4717.

(25) D'Amore, C.; Di Leva, F. S.; Sepe, V.; Renga, B.; Del Gaudio, C.; D'Auria, M. V.; Zampella, A.; Fiorucci, S.; Limongelli, V. Design, synthesis, and biological evaluation of potent dual agonists of nuclear and membrane bile acid receptors. *J. Med. Chem.* **2014**, *57*, 937-954.

(26) Kaplowitz, N. Acetaminophen hepatoxicity: what do we know, what don't we know, and what do we do next? *Hepatology* **2004**, *40*, 23-26.

(27) McGill, M. R.; Jaeschke, H. Metabolism and disposition of acetaminophen: recent advances in relation to hepatotoxicity and diagnosis. *Pharm Res*. **2013**, *30*, 2174-2187.

(28) Lee, F. Y.; de Aguiar Vallim, T. Q.; Chong, H. K.; Zhang, Y.; Liu, Y.; Jones, S. A.; Osborne, T. F.; Edwards, P. A. Activation of the farnesoid X receptor provides protection against acetaminophen-induced hepatic toxicity. *Mol Endocrinol*. **2010**, *24*, 1626-1636.

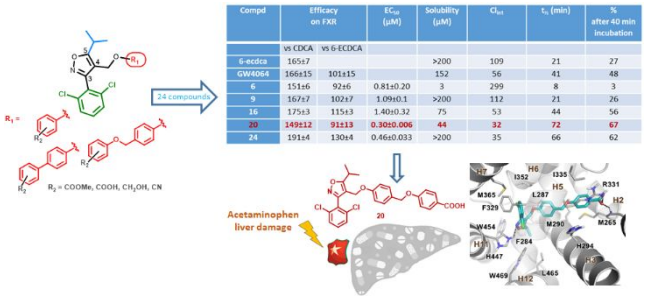

Compd	Efficacy on FXR		EC_{50} (μM)	Solubility (μM)	Cl_{int}	$t_{1/2}$ (min)	% after 40 min incubation
	vs CDCA	vs 6-ECDCA					
6-ecdca	165±7			>200	109	21	27
GW4064	166±15	101±15		152	56	41	48
6	151±6	92±6	0.81±0.20	3	299	8	3
9	167±7	102±7	1.09±0.1	>200	112	21	26
16	175±3	115±3	1.40±0.32	75	53	44	56
20	149±12	91±13	0.30±0.006	44	32	72	67
24	191±4	130±4	0.46±0.033	>200	35	66	62